Noname manuscript No.
(will be inserted by the editor)

LowCOST-HSQC variants for fast pulsing high ω_1-resolved 2D-experiments

David Schulze-Sünninghausen[1] · **Johanna Becker**[2] · **Martin R. M. Koos**[3] · **Burkhard Luy**[4,*]

Received: date / Accepted: date

Abstract The LowCOST-HSQC is a sensitivity-enhanced HSQC version that retains unused proton polarization for subsequent scans in correlations to low natural abundance nuclei like ^{13}C or ^{15}N. Together with fast polarization distribution via isotropic mixing, it allows the acquisition of fast pulsing 2D-experiments. We give a detailed introduction and comparison of three possible INEPT-type transfer elements for the LowCOST approach – the original LowCOST, the ZIP, and a specific TIG-BIRD element – and evaluate various variants of the LowCOST-HSQC.

Keywords Fast pulsing 2D NMR · LowCOST · ASAP · ZIP · HSQC · TIG-BIRD

[1]David Schulze-Sünninghausen
Bruker BioSpin GmbH & Co. KG
Rudolf-Plank-Str. 23
76275 Ettlingen
Germany
[2]Johanna Becker
Currenta GmbH & Co. OHG
Analytik
51368 Leverkusen
Germany
[3]Martin R. M. Koos
Pfizer Incorporated
06340 Groton
Connecticut, USA
[4]Burkhard Luy*
Institute of Organic Chemistry and
Institute for Biological Interfaces 4 - Magnetic Resonance
Karlsruhe Institute of Technology (KIT)
Hermann-von-Helmholtz-Platz 1
76344 Eggenstein-Leopoldshafen
Germany
Tel.: +49 721 608 29360 (B.L.)
E-mail: burkhard.luy@kit.edu
ORCID-ID: 0000-0001-9580-6397
*corresponding author

1 Introduction

Fast pulsing 2D experiments have demonstrated their incredible performance. Starting from the revolution in protein-NMR, where the FAST and SO-FAST experiments [1–3] as well as the many different BEST experiments [4–6] lead to a vast reduction in measurement times, Ernst-angle excitation [7–9] and fast TOCSY-type equilibration [10, 11] in 2D heteronuclear correlation experiments have dramatically increased the possibilities also in small molecule NMR. The best one-bond correlation experiment with acquisition times down to a couple of seconds is the ASAP-HSQC [12, 13] and its variants [13–16]. The approach also allows the acquisition of HSQCs with a ω_1-resolution down to 0.5 Hz in less than ten minutes [13]. However, sensitivity-enhancement as a well-known strategy to combine echo/antiecho detection schemes with utmost sensitivity is not compatible with the approach. Furthermore, a detailed analysis revealed that unused polarization is in the transverse plane during t_1 increments and evolves homonuclear couplings, thereby reducing the accessible reservoir polarization significantly. The search for a fast pulsing HSQC variant tolerating sensitivity enhancement, the LowCOST-HSQC [17] as well as the ZIP-HSQC [18, 19] have been developed independently, leading to sequences following the same underlying principle that differ only in the specific extension of the INEPT-type forward transfer element.

In the following, we will first compare the two transfer elements and a third one resembling a TIG-BIRD implementation [20, 21], before we introduce several extensions to the sequence. We then provide a constant time version, a BIRD^r variant with multiplicity editing and decoupling of long-range heteronuclear couplings in the indirect dimension, and an HSQC-TOCSY type experiment. All sequences are enhanced by broadband shaped pulses and demonstrated on small molecule examples.

2 Results and Discussion

Conventional HMQC- and HSQC-type experiments detect ^{13}C-bound proton magnetization, but effectively dephase all unused ^{1}H magnetization not directly bound to ^{13}C nuclei. As a consequence, only T_1-relaxation can build up polarization for the next scan, leading inevitably to long recovery delays d_r between scans. The ALSOFAST and ASAP approaches [9, 10, 12, 13] for HMQC/HSQC experiments retain the unused magnetization and allow a much faster recovery via Ernst-angle-type excitation and isotropic mixing based redistribution of polarization. In this way, experiment times are reduced dramatically, allowing acquisitions of 2D experiments in less than three seconds or the recording of highly ω_1-resolved 2D-HSQC spectra on the order of minutes. Particularly, the ASAP-HSQC provides short, high-quality spectra with enhanced sensitivity compared to conventional HSQC spectra for a given measurement time. However, for experiments with many increments the sensitivity of spectra not always reaches the desired improvement.

The known downside of the ASAP-HSQC approach and the cause of signal reduction at long acquisition times in the indirect dimension is the orientation of unused magnetization in the transverse plane during the t_1-evolution period. If the acquisition time in the indirect dimension is chosen to be long, ^{1}H-^{1}H couplings may evolve, converting spin polarization into coherence unaccessible in following scans. This problem also persists in protein-NMR, where the water needs to be controlled to maximize sensitivity in subsequent scans of exchanging amide protons.

One way to solve this issue in protein-NMR was developed in the COST-HSQC (Cooling Overall Spin Temperature-HSQC) [22]: Using selective pulses, magnetization is prepared in such a way, that ^{15}N-coupled protons polarization is transferred to heteronuclear antiphase magnetization ($I_z \rightarrow 2I_zS_x$), while at the same time heteronuclear uncoupled polarization is reoriented along z ($I_z \rightarrow I_z$). With this trick, not only unused spin polarization is safely stored during t_1, but also sensitivity enhancement can be applied, which will result in uncoupled magnetization being repositioned along z during acquisition, as the homonuclear part of the sensitivity enhancement sequence represents a perfect echo [23] with inherent planar mixing Hamiltonian. While the original idea is to enhance sensitivity via chemical exchange of amide protons with alread polarized water, it may also serve in other ways as a polarization reservoir for the next scan.

It would be good to have a COST-like approach available for small molecule NMR. But in most applications with natural abundance samples, band-selective treatment using shaped pulses is not possible. The obvious choice, instead, would be the application of bilinear rotations like the BIRD-element [**?**], which treats ^{13}C-bound spins different from other protons. In the LowCOST-HSQC [17] as well as in the ZIP-HSQC [18], two different elements have been proposed that lead to the desired transfer. While Ernst-angle-type excitation is not compatible with the approach, ASAP-type isotropic mixing for fast polarization redistribution is possible and can be combined with sensitivity enhancement. Next to the two sequences, a third transfer element exists (mentioned already in [19]), as the transfer problem resembles that of the TIG-BIRD approach [21] or a BIG-BIRD element [20] with a subsequent INEPT-step.

2.1 Comparison of forward-transfer elements

The three different forward-transfer pulse sequence elements are shown together with a conventional INEPT in Fig. 1 in hard pulse (A-D) and shaped pulse variants (A'-D'). While the conventional INEPT has a single refocused delay of duration $2\Delta = 1/(2J)$, where the nominal coupling constant is typically set to an intermediate value of J=145 Hz. All three bilinear rotation type transfer elements require coupling evolution periods with an overall duration of 6Δ. However, the sequences apply four (LowCOST), three (ZIP), and two (TIG-BIRD) 180° hard pulses on the heteronucleus, which are known to have a severe offset dependence. It is therefore hardly surprising that the evaluation of corresponding hard pulse sequences shows dramatic losses at larger offsets for all three implementations with particular losses for the LowCOST variant. It is therefore an obvious choice to replace hard pulses by offset compensated broadband pulse shapes. Using optimal control theory, a large multitude of such shaped pulses has been developed over the last two decades [24–35], with the BUBI pulse sandwich sticking out, as it is compensated for J-coupling evolution during simultaneously applied shapes [36, 37]. The shaped pulse sequences with pictograms are given in Fig. 1 together with specific pulse shapes stated in the figure caption. With the application of broadband pulses with compensated ^{13}C and ^{1}H frequency ranges of 37.5 kHz and 10 kHz, respectively, the transfer efficiency of all three elements changes significantly, leading to essentially identical and highly improved performance. Consequently, any of the shaped pulse elements may be used in the experiment variants that will be introduced in the following paragraphs and a placeholder is put for any of the forward-transfer element.

2.2 Comparison of LowCOST- and ASAP-HSQC

The ASAP-HSQC experiment has been studied extensively in both theory and experiment during the last decade [12–16]. It uses Ernst-angle-type excitation and isotropic mixing based fast polarization redistribution to significantly enhance sensitivity, but also comes with the caveat that it is

generally not compatible with sensitivity enhanced back-transfer. The LowCOST-HSQC and the ZIP-HSQC, instead, provide fast polarization redistribution and sensitivity enhanced back-transfer, but are incompatible with Ernst-angle-type excitation. In addition, the already mentioned storage of reservoir magnetization during t_1 is profoundly different: while ALSOFAST- and ASAP-HSQCs store the reservoir as transverse coherence, LowCOST- and ZIP-HSQCs store the reservoir as polarization along z, effectively avoiding coupling evolution for ^{1}H,^{1}H-couplings in the weak coupling limit. Different spin systems and experimental settings will therefore react differently to the fast pulsing approaches.

In Fig. 3 the resulting effects on sensitivity are measured on the test molecule menthol, which provides a number of different spin system properties. Basic ASAP-HSQC and LowCOST-HSQC experiments using broadband shaped pulses have been recorded with 15% NUS (non uniform sampling) and different numbers of t_1-increments and therefore different acquisition times in the indirect dimension.

We can distinguish two extremes of spin systems for menthol: The methyl groups, for which the signal itself comes from three spins, while only one nearest neighbor atom serves as the main spin reservoir, and all other CH or CH_2 groups, where one or two recorded protons have a minimum of four directly coupled neighboring spins. All spins have relaxation times in the range of 1-2 seconds, providing very little recovery between scans within the very short interscan delays d_r of ≈100 ms. As expected from theory (see [16] for a thorough theoretical treatment), the three methyl groups (uppermost intensive signals in the spectra of Fig. 3) show relatively low intensities in the LowCOST-HSQC spectra compared to the ASAP-HSQC. The effect is stronger for short acquisition times and less pronounced for the longest acquisition time applied. Apparently, isotropic mixing spin redistribution has little effect for methyl groups with their small spin reservoir and the dominating effect of polarization recovery is provided by the Ernst-angle-type excitation in the ASAP-HSQC. Even sensitivity enhancement in the LowCOST-HSQC cannot counteract this advantage for the ASAP-HSQC. For long acquisition times, however, the improvement is to some extent outweighed by the reservoir storage along z during t_1 in the LowCOST-HSQC, as coupling evolution in the ASAP-HSQC reduces the reservoir polarization for long t_1 increments even for the case of a single directly coupled proton.

The situation is very different for all other protons in the other spin systems: the large coupling networks lead to effective redistribution of spin polarization and sensitivity enhancement is sufficient to provide better signal-to-noise for the LowCOST-HSQC as compared to the ASAP-HSQC. The advantage for the LowCOST-HSQC significantly increases even for long acquisition time due to the favorable storage of reservoir polarization along z, which has a particularly dramatic effect for the heavily coupled spins.

2.3 Constant Time LowCOST-HSQC

In Fig. 2 C a constant time version of the LowCOST-HSQC is given. The constant time ensures equal relaxation behavior during t_1 incrementation and, depending on the overall constant time period 2τ, it is able to refocus potential ^{13}C,^{13}C-couplings in fully or partially isotope-labeled samples. For fully isotope-labeled small molecules the LowCOST-approach does not make sense, as it relies on detected heteronuclei to be at low abundance. In fluxomics-type studies, where only local isotope-labeling is expected for a small percentage of molecules, the constant time LowCOST-HSQC can be of interest for boosting sensitivity. However, as we do not have access to this type of sample in our laboratory, we can only mention this potential type of application. Instead, we focus on the enhancement in natural abundance samples compared to a conventional constant time HSQC with sensitivity enhancement when fast pulsing, i.e. short overall experimental times, is required. Example spectra are shown in Fig. 4 for menthol. For the applied recovery delay d_r=100 ms, a clear improvement in intensity for all signals but the isolated methyl groups is found. This improvement can almost exclusively be attributed to the isotropic mixing based redistribution of spin polarization, which also explains why the methyl groups with their small effective spin systems do not benefit from the LowCOST approach.

2.4 LowCOST-BIRD^r-HSQC

It has been clearly demonstrated in a number of publications [38–41], that the application of a BIRD^r filter element [42, 43] in the center of t_1 provides a reduced multiplet structure in the indirect dimension that can be highly useful for the measurement of heteronuclear one-bond couplings. A corresponding LowCOST-BIRD^r-HSQC sequence is given in Fig. 2 D.

A comparison of an ω_1-coupled LowCOST-HSQC and the LowCOST-BIRD^r-HSQC is shown in Fig. 5. Clearly the BIRD^r-enhanced spectrum provides significantly reduced multiplet widths with increased sensitivity and therefore simplifies the determination of one-bond couplings. However, as coupling measurements have to be performed in the indirect dimension, overall measurement times may become very long due to the large number of necessary t_1 increments. As a consequence, the LowCOST approach and the application of NUS seems to be particularly favorable. Corresponding example spectra for norcamphor are shown in Fig. 6 for conventional acquisition with 8192 increments and for the same resolution acquired with 15% NUS. Previous

studies mention that the influence of NUS on the accuracy of coupling measurement is negligible and although we did not attempt a detailed evaluation of data, a qualitative visual inspection did not show any differences for the two acquisition schemes. The only effect we could observe was a slight expected decrease in sensitivity due to the reduced number of actually recorded increments.

2.5 LowCOST-HSQC-TOCSY

As has been pointed out for the ASAP-HSQC-TOCSY [15], the isotropic mixing sequence does not need to be applied additionally at the beginning of an experiment for efficient and fast redistribution of spin polarization, but if the right type of isotropic mixing multiple pulse sequence is used, it can be combined with a conventional TOCSY period at the end of a 2D acquisition scheme right before the acquisition of individual FIDs. The corresponding pulse sequence for a LowCOST-HSQC-TOCSY is provided in Fig. 2 E. The preferred isotropic mixing case in our laboratory is the classical DIPSI-2 multiple pulse sequence [44], which guarantees isotropic mixing conditions along all three axes with a bandwidth that roughly corresponds to the applied rf-amplitude. The latter is a prerequisite for the LowCOST-HSQC-TOCSY, as TOCSY-transfer with the detected magnetization occurs in the transverse plane, while redistribution of reservoir magnetization happens along z.

Example spectra for a comparison with fast pulsing conventional experiments are given in Fig. 7. The upper two experiments were acquired with exactly identical overall experiment times of 19 s and are trimmed for minimum measurement time for the experiment. Please be aware that no NUS was applied and 128 increments together with 4 dummy scans were acquired in 19 s. The recovery delay has been minimized and is determined by technical boundaries like the time needed for disc I/O. Overall acquisition time plus minimum delays add up to an effective recovery time on the order of 100 ms. Under these conditions the conventional HSQC-TOCSY provides spectra of remarkable performance, but the LowCOST-HSQC-TOCSY shows significantly enhanced sensitivity exceeding a factor of 3 for some resonance. Also spectral artefacts are reduced. Bottom two spectra have been acquired with longer acquisition times in the direct dimension and an overall effective recovery time on the order of 250 ms. Clearly, the enhanced resolution benefits the spectral quality with a still fast experiment time of 43 s. The improvement in sensitivity of the LowCOST-TOCSY is comparable.

3 Conclusion

Following the original COST-HSQC designed for ^{15}N-labeled proteins [22], a transfer element that specifically produces $2I_zS_y$ for heteronuclear coupled IS spins, while maintaining I_z polarization for uncoupled I spins, has been developed that allows the storage of unused polarization along z during t_1 periods and together with sensitivity enhanced back-transfer its conservation for the following scan. Particularly in fast pulsing experiments this approach guarantees fast repetition rates with isotropic mixing polarization distribution as introduced with the ASAP-HMQC [10]. Equivalent approaches have been developed independently in the LowCOST-HSQC [17] and the ZIP-HSQC [18, 19]. As the LowCOST-HSQC was reported earlier, we use the term LowCOST-HSQC throughout this article, while it could also be termed ZIP-HSQC.

The core of the experiment is the forward transfer element, for which three different versions do exist. The original LowCOST version is not really optimized and requires four carbon inversion pulses, while the ZIP-element requires only three carbon inversions and the TIG-BIRD transfer element only two. But in the original LowCOST implementation already the use of compensated optimal control derived pulse shapes has been suggested. The three elements are thoroughly studied here with respect to their transfer properties as hard pulse as well as broadband compensated shaped pulse versions. Clearly, ZIP and TIG-BIRD hard pulse versions provide better results than the LowCOST transfer element. Their overall performance, however, is generally bad and the application of hard pulses should only be considered up to 400 MHz spectrometers. For higher spectrometer fields, the use of shaped pulses is highly recommended. The compensated pulse versions of the three transfer elements essentially provide equivalent results and can be exchange at will in all experiments shown. However, the TIG-BIRD sequence uses the least amount of pulses and therefore the least amount of rf-energy, which is beneficial especially in fast pulsing experiments. We therefore recommend the offset-compensated TIG-BIRD sequence. It should be noted, that the supporting information of [19] contains a study that clearly favors the ZIP-element over a TIG-BIRD element. The TIG-BIRD sequence used ($45^\circ_{315} - \Delta - 180^\circ_x - \Delta - 45^\circ_{135}$ instead of $45^\circ_{315} - \Delta - 180^\circ_{315} - \Delta - 90^\circ_{225}$ used here), however, is wrongly derived and must lead to reduced transfer, which also explains the contradicting result.

When comparing ALSOFAST, ASAP and LowCOST as the most preferential versions of reservoir-retaining HSQCs for small molecules, four aspects can be identified for the three classes of experiments that influence the resulting sensitivity improvement: i) Ernst-angle-type excitation, which is applied in ALSOFAST/ASAP experiments, but is not compatible with the LowCOST approach; ii) the classical sensi-

Table 1: Fast pulsing HSQC approaches and their enhancement factors.

	ALSOFAST	**ASAP**	**LowCOST/ZIP**	**benefitting spins**
Ernst-angle-type excitation	✓	✓	—	all slow relaxing spins
sensitivity-enhanced back-transfer	—	—	✓	all multiplicities $CH_2 > CH_3 > CH$
fast isotropic mixing redistribution	—	✓	✓	large effective spin systems
magn. reservoir along z during t_1	—	—	✓	spins with large multiplets
best overall performance	isolated spins only	short overall experiment times	long ω_1 acquisition times	

tivity enhanced back-transfer, on the other hand, is used in LowCOST experiments, but is not compatible with ALSOFAST/ASAP sequences; iii) the fast isotropic mixing redistribution of spin polarization is provided in ASAP and LowCOST experiments, but not in ALSOFAST-type approaches; and iv) the suppression of ^{1}H,^{1}H-coupling evolution during t_1 is beneficial in LowCOST experiments, but not campatible with either ALSOFAST and ASAP approaches. The approaches are also summarized in Table 1.

This leads to classification regarding the expected benefits for the different approaches: The ALSOFAST approach is only favorable for isolated spins for which the Ernst-angle-type excitation is the only way to improve sensitivity. The ASAP-HSQC combines the Ernst-angle-type excitation with fast isotropic mixing polarization redistribution, leading to best results for small spin systems with relatively little reservoir and short acquisition times in the indirect dimension. The LowCOST approach increases its performance with the number of directly coupled and even more with the applied acquisition time in the indirect dimension. As such, LowCOST-type experiments are clear favorites for experiments that target utmost resolution in the indirect dimension, while very short experiments with very few t_1 increments are preferrably run as ASAP-type experiments.

The constant time LowCOST-HSQC, LowCOST-BIRD$'$-HSQC, and LowCOST-HSQC-TOCSY experiments provided here are the logic extensions for fast pulsing heteronuclear correlation experiments provided in their ALSOFAST/ASAP version in [13–15].

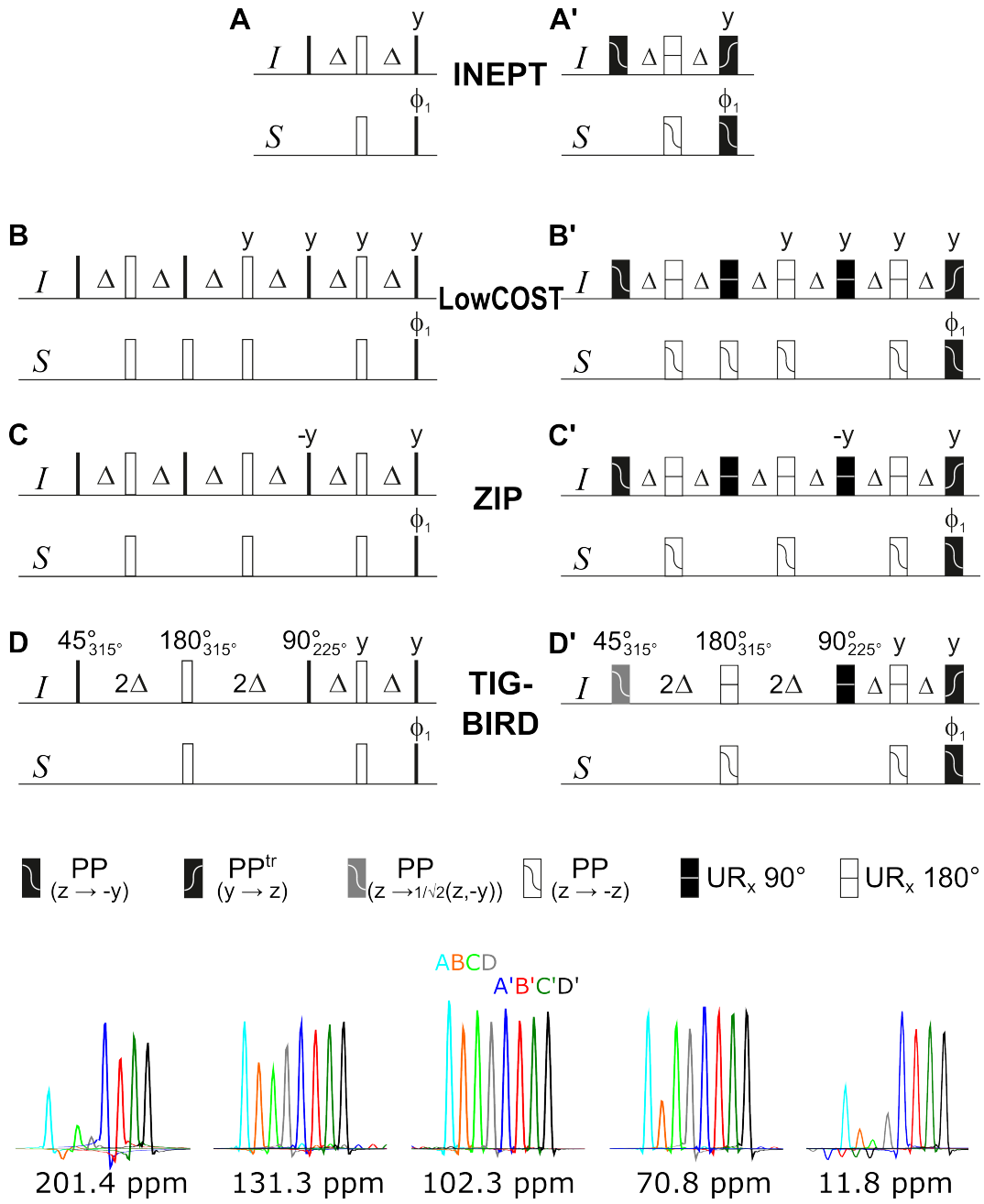

Fig. 1: INEPT (A,A') and three versions of forward transfer into $2I_zS_y$ antiphase for heteronuclear coupled spins that at the same time align uncoupled spins for storage as I_z polarization during t_1 delays: the original LowCOST transfer element (B,B'), the ZIP-element (C,C'), and the corresponding TIG-BIRD sequence (D,D'). Sequences indicated with simple letters are hard pulse versions, while letters with a prime mark the corresponding versions with broadband shaped pulses. The delay is set to $\Delta = 1/(4J)$ with a nominal one-bond coupling J. 90° hard pulses are indicated by solid bars, open bars refer to 180° hard pulses. Phases are along x unless indexed otherwise. The pictograms for shaped pulses are explained below the sequences, where PP corresponds to point-to-point pulses with start and final orientations of spin components as mentioned in parentheses and UR represents universal rotation pulses with the corresponding rotation angle in degrees. All pulses are applied along x unless indicated otherwise. Pulses indicated in degrees with subscript phases in degrees are used if phases differing from Cartesian axes are required. Actual pulse shapes used for experiments have been derived from optimal control theory based optimizations. For PP($z \rightarrow -y$) and PP($y \rightarrow z$) pulses as well as UR180(^{1}H) and PP($z \rightarrow$ -z)(^{13}C), the individual pulse shapes of J-compensated BEBE^{tr} and BUBI pulse sandwiches [36] are applied. The ^{13}C UR 180° pulse shape is constructed from two corresponding PP($z \rightarrow -y$) shapes following the construction principle [45]. The pulse with an effective flip angle of 45° has been developed for INADEQUATE applications and will be published elsewhere [46]. Resulting intensities in LowCOST-HSQC experiments with corresponding forward transfer elements are shown for a number of cross peaks with ^{13}C chemical shifts as indicated. An approximately 100 mM sample of hydroquinidine and acetaldehyde dissolved in DMSO-d_6 was used on a 600 MHz spectrometer.

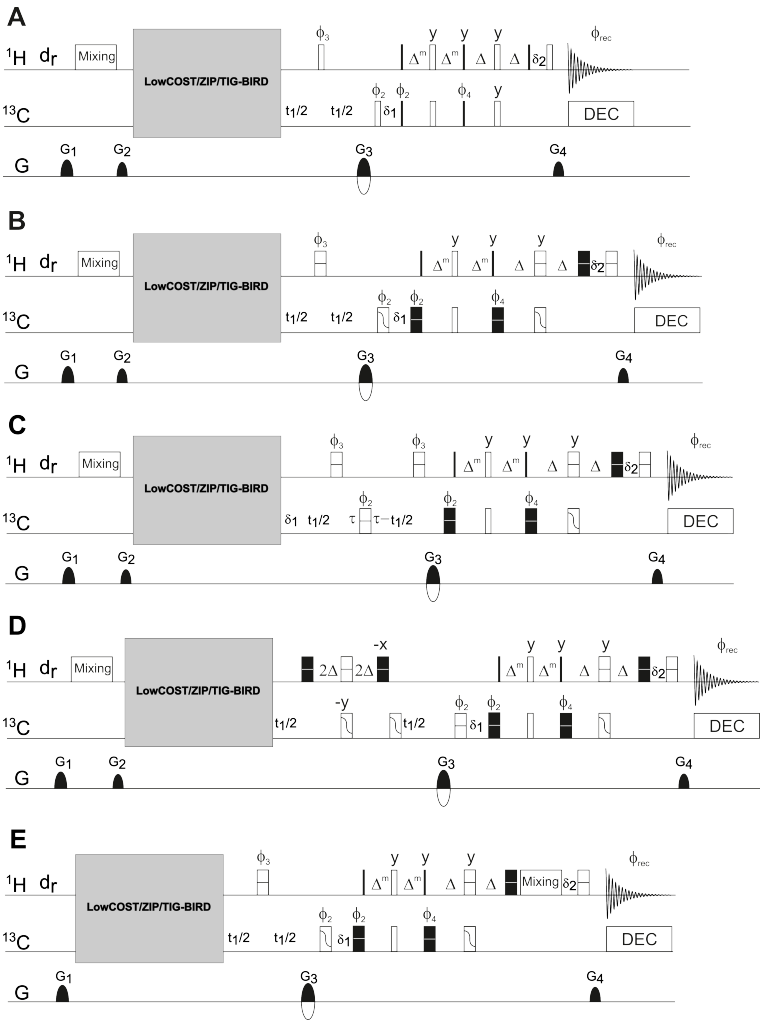

Fig. 2: Pulse sequences compilation: Hard pulse LowCOST-HSQC (A), broadband shaped pulse LowCOST-HSQC (B), constant-time LowCOST-HSQC (C), LowCOST-BIRD^r-HSQC (D), and LowCOST-HSQC-TOCSY (E). 90° hard pulses are indicated by thin filled bars, while hard 180° pulses are represented by open bars. All point-to-point and universal rotation shaped pulses are used as defined in the caption of Fig. 1. As *J*-compensated pulse sandwiches with a universal rotation 90° pulses are not yet available, corresponding ^{1}H pulses are applied as hard pulses. For rf-energy reasons hard 180° pulses are also applied in cases where two simultaneous universal rotation pulses are required, although also *J*-compensated BUBU pulse sandwiches [37] may be applied. Big gray boxes indicate the forward transfer placeholder, for which one of the transfer elements of Fig. 1 has to be filled in. Pulse phases are along x unless indicated otherwise. $\phi_1 = x,-x$, $\phi_2 = x,x,-x,-x$, $\phi_3 = -y,-y,y,y$, $\phi_4 = -y,-y,-y,-y,y,y,y,y$, $\phi_{\mathrm{rec}} = x,-x,-x,x$. Gradients are $G_1 = 31\%$, $G_2 = 17\%$, $G_3 = 80\%$, and $G_4 = 20.1\%$, where the sign of G_3 is changed with echo/antiecho selection together with phase ϕ_5. Delays δ_1 and δ_2 need to be adjusted so that initial t_1 increments are effectively set to zero and the magnetization is fully refocused before acquisition. DIPSI-2 is used whenever a Mixing period is indicated in the sequences and standard adiabatic ca-WURST decoupling is applied during acquisition. Recovery delays d_r are varied as described with actual acquired spectra.

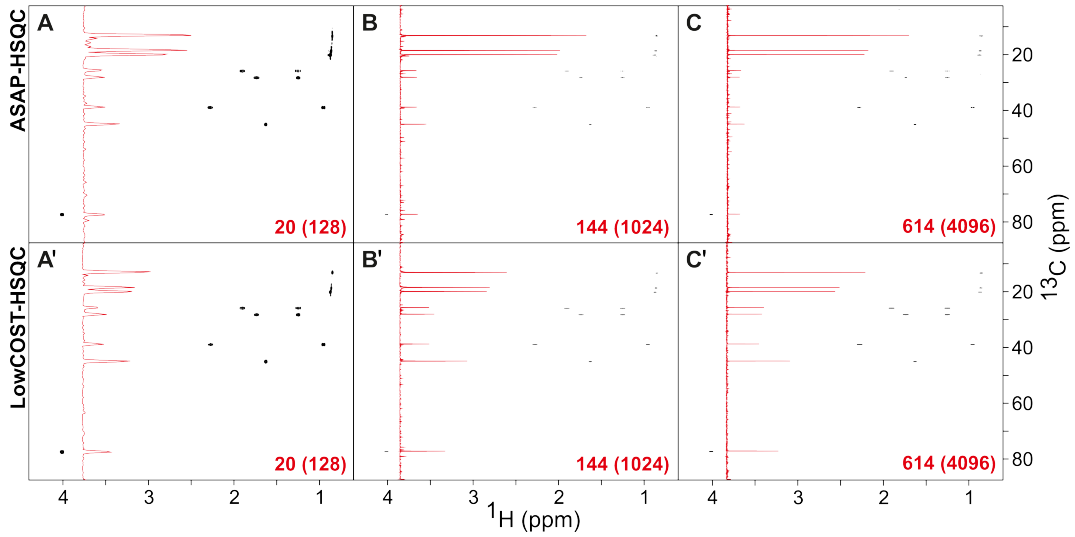

Fig. 3: Comparison of ASAP-HSQC (A-C) and LowCOST-HSQC (A'-C') spectra for three different ^{13}C resolutions acquired on 500 mM borneol. All spectra were acquired with 512 points in the directly detected dimension, resulting in a ^{1}H acquisition time of 112.4 ms. Recovery delays on the order of 100 ms were applied with a fine adjustment of the ASAP-HSQC delay for the same overall duration. In all cases 15% NUS was applied, leading to 20(256), 144(1024), and 614(4096) acquired (and NUS-processed) data points, and to acquisition times of 5 ms (A,A'), 39.9 ms (B,B') and 159.8 ms (C,C'), respectively. After processing with linear prediction and zero filling, ^{13}C digital resolutions of 50.1 Hz (A,A'), 6.26 Hz (B,B'), and 1.57 Hz (C,C') were obtained in overall experiment times of 9 s, 51 s, and 3 min 46 s, respectively. Spectra are displayed with identical settings. The projections along the ^{13}C dimensions are given as inserts in red for each spectrum.

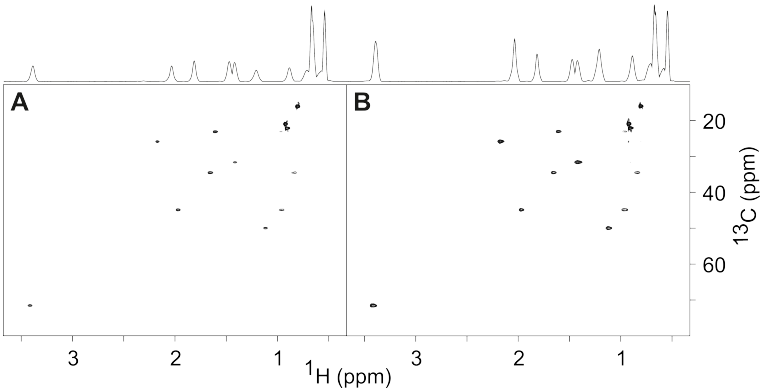

Fig. 4: Comparison of two constant time LowCOST-HSQC spectra for demonstrating the effect of isotropic mixing based redistribution of polarization. Spectra are recorded with a relaxation delay d_r=34.54 ms (A) and no specified relaxation delay but a DIPSI-2 isotropic mixing period of equal length and otherwise identical settings (B). The constant time delay was set to $2\tau = 12$ ms. Spectra were acquired with 256 (^{1}H) $\times$ 128 (^{13}C) points and resulting acquisition times of 63.7 ms and 6.06 ms, respectively. After processing with linear prediction and zero filling digital resolution of 3.92 Hz and 41.21 Hz, respectively, were achieved. The overall duration with one scan per increment and four dummy scans was 18 s. Clearly, the improved sensitivity for non-methyl groups is visible.

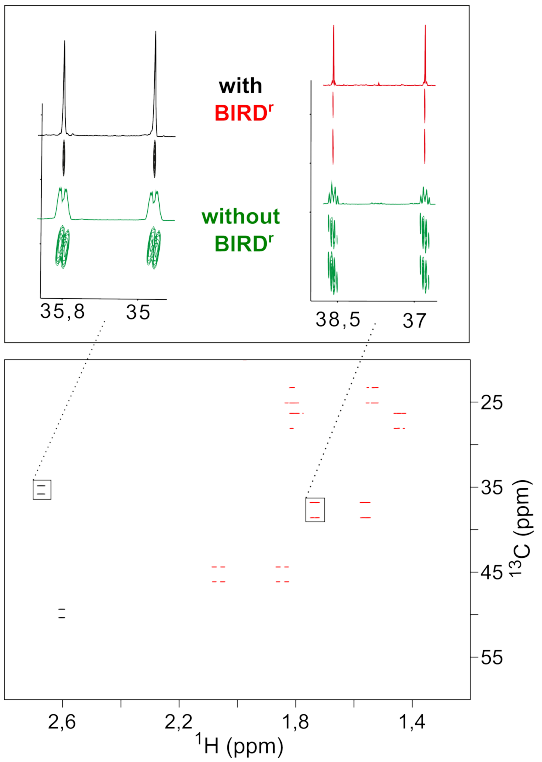

Fig. 5: A ω_1-coupled LowCOST-BIRD^r-HSQC spectrum acquired using sequence Fig. 2 D (bottom) and the comparison of example cross peaks with a ω_1-coupled LowCOST-HSQC without BIRD^r element (top) measured on norcamphor. The BIRD^r filter element effectively decouples ^{1}H,^{1}H-couplings in the indirect dimension and also acts as a multiplicity editing element in which CH and CH_3 groups appear with positive cross peaks (black), while CH_2 groups are inverted (red). In th top part the reference cross peaks of the ω_1-coupled LowCOST-HSQC without BIRD^r element are shown in green. Clearly, the decoupling effect is visible. Spectra were acquired with 512 (^{1}H) $\times$ 4096 (^{13}C) points and resulting acquisition times of 266.9 ms and 339.5 ms, respectively. In addition, linear prediction and zero filling were applied, which results in a final digital resolution of 0.94 Hz (^{1}H) and 0.74 Hz (^{13}C), respectively. With a recovery delay d_r=100 ms, 16 dummy scans, and 1 scan per t_1 increment the overall measurement time resulted in 42 minutes per spectrum.

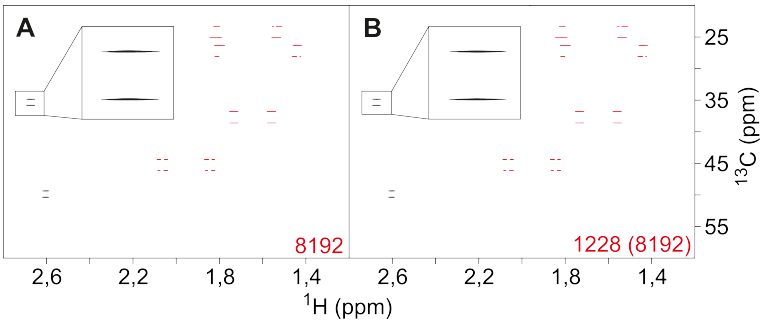

Fig. 6: Comparison of ω_1-coupled LowCOST-BIRD^r-HSQC spectra acquired conventionally (A) and using 15% NUS reduction for the indirect dimension (B). The sequence from Fig. 2 D has been used in both cases using norcamphor as a test compound. Spectra were acquired with 256 (^{1}H) $\times$ 8192 (^{13}C) points and resulting acquisition times of 133.5 ms and 679 ms, respectively. Linear prediction and zero filling were applied in both dimensions and in addition to NUS sampling for spectrum B, which results in a final digital resolution of 1.87 Hz (^{1}H) and 0.37 Hz (^{13}C), respectively. With a recovery delay d_r=50 ms, 16 dummy scans, and 1 scan per t_1 increment the overall measurement time resulted in 1 h 21 min (A) and 11 min 49 s (B). Spectra are virtually identical.

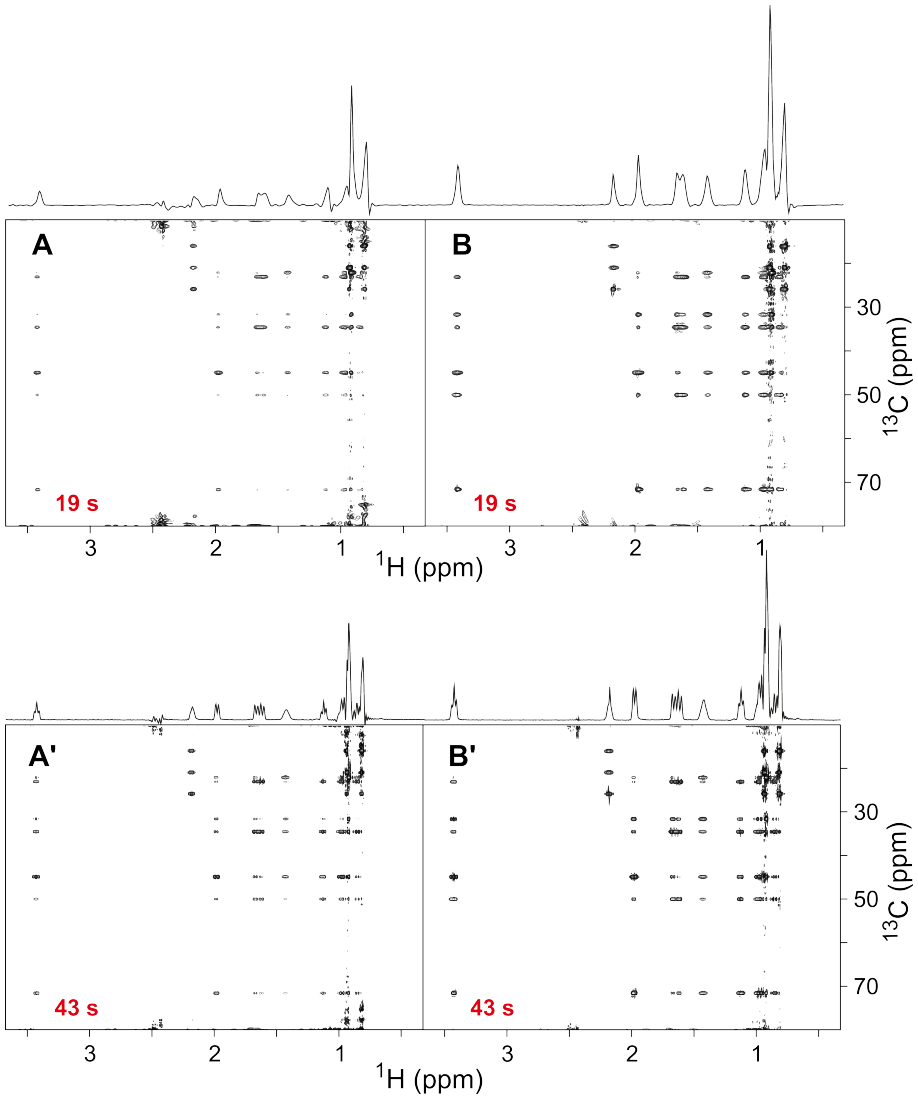

Fig. 7: Comparison of conventional and LowCOST HSQC-TOCSY spectra under fast pulsing conditions. A conventional TOCSY with sensitivity enhanced back-transfer [47–52] (A,A'), as well as the LowCOST-HSQC-TOCSY provided in Fig. reffig2 E (B,B'). The top two spectra (A,B) were acquired with 256 (^{1}H) × 128 (^{13}C) points with acquisition times of 63.7 ms and 6.06 ms, respectively. the recovery delay was set to the shortest possible writing delay on our Bruker spectrometer (30 ms) plus a small correction for the conventional HSQC-TOCSY to provide exactly identical overall experiment times of 19 s for the two compared spectra. Bottom spectra (A',B') were acquired with higher resolution in the directly detected dimension with 512 (^{1}H) × 128 (^{13}C) points and acquisition times of 127.5 ms and 6.06 ms, respectively. In addition, the recovery delay was increased by 100 ms compared to the upper spectra. The settings result in exactly identical overall experiment times of 43 s. For isotropic mixing the DIPSI-2 sequence with a mixing time of 34.54 ms was applied. Data were processed using linear prediction and zero filling in the direct dimension, leading to ^{1}H digital resolutions of 3.92 Hz (A,B) and 1.96 Hz (A',B'), respectively. Positive projections are provided at the top of 2D spectra to indicate relative signal intensities.

4 Acknowledgements

B.L. gratefully thank the Deutsche Forschungsgemeinschaft (DFG SFB 1527 HyPERION, project C01) and the HGF-programme Information (45.35.02) for financial support.

References

1. A. Ross, M. Salzmann, H. Senn, J Biomol NMR **10**(4), 389 (1997). DOI 10.1023/A:1018361214472
2. P. Schanda, Ē. Kupče, B. Brutscher, J Biomol NMR **33**(4), 199 (2005). DOI 10.1007/s10858-005-4425-x
3. P. Schanda, B. Brutscher, J. Am. Chem. Soc. **127**(22), 8014 (2005). DOI 10.1021/ja051306e
4. P. Schanda, H. Van Melckebeke, B. Brutscher, J. Am. Chem. Soc. **128**(28), 9042 (2006). DOI 10.1021/ja062025p
5. E. Lescop, P. Schanda, B. Brutscher, Journal of Magnetic Resonance **187**(1), 163 (2007). DOI 10.1016/j.jmr.2007.04.002
6. J. Farjon, J. Boisbouvier, P. Schanda, A. Pardi, J.P. Simorre, B. Brutscher, J. Am. Chem. Soc. **131**(24), 8571 (2009). DOI 10.1021/ja901633y
7. R.R. Ernst, W.A. Anderson, Review of Scientific Instruments **37**(1), 93 (1966). DOI 10.1063/1.1719961
8. R.R. Ernst, in *Advances in Magnetic and Optical Resonance*, vol. 2, ed. by J.S. Waugh (Academic Press, 1966), pp. 1–135. DOI 10.1016/B978-1-4832-3115-0.50008-9
9. L. Mueller, J Biomol NMR **42**(2), 129 (2008). DOI 10.1007/s10858-008-9270-2
10. E. Kupče, R. Freeman, Magnetic Resonance in Chemistry **45**(1), 2 (2007). DOI 10.1002/mrc.1931
11. J. Furrer, Chem. Commun. **46**(19), 3396 (2010). DOI 10.1039/C000964D
12. D. Schulze-Sünninghausen, J. Becker, B. Luy, J. Am. Chem. Soc. **136**(4), 1242 (2014). DOI 10.1021/ja411588d
13. D. Schulze-Sünninghausen, J. Becker, M.R.M. Koos, B. Luy, J Magn Reson **281**, 151 (2017). DOI 10.1016/j.jmr.2017.05.012
14. J. Becker, B. Luy, Magnetic Reson in Chemistry **53**(11), 878 (2015). DOI 10.1002/mrc.4276
15. J. Becker, M.R.M. Koos, D. Schulze-Sünninghausen, B. Luy, Journal of Magnetic Resonance **300**, 76 (2019). DOI 10.1016/j.jmr.2018.12.021
16. M.R.M. Koos, B. Luy, Journal of Magnetic Resonance **300**, 61 (2019). DOI 10.1016/j.jmr.2018.12.014
17. D. Schulze-Sünninghausen, Entwicklung und Optimierung schneller mehrdimensionaler NMR-Experimente. Ph.D. thesis, Karlsruher Institut für Technologie (KIT), Karlsruhe, Germany (2016)
18. Ē. Kupče, L. Frydman, A.G. Webb, J.R.J. Yong, T.D.W. Claridge, Nat Rev Methods Primers **1**(1), 1 (2021). DOI 10.1038/s43586-021-00024-3
19. J.R.J. Yong, A.L. Hansen, Ē. Kupče, T.D.W. Claridge, Journal of Magnetic Resonance **329**, 107027 (2021). DOI 10.1016/j.jmr.2021.107027
20. J. Briand, O.W. Sørensen, J Magn Reson **125**(1), 202 (1997). DOI 10.1006/jmre.1996.1095
21. J. Briand, O.W. Sørensen, J Magn Reson **135**(1), 44 (1998). DOI 10.1006/jmre.1998.1556
22. M. Deschamps, I.D. Campbell, Journal of Magnetic Resonance **178**(2), 206 (2006). DOI 10.1016/j.jmr.2005.09.011
23. K. Takegoshi, K. Ogura, K. Hikichi, Journal of Magnetic Resonance (1969) **84**(3), 611 (1989). DOI 10.1016/0022-2364(89)90127-3
24. T.E. Skinner, T.O. Reiss, B. Luy, N. Khaneja, S.J. Glaser, J Magn Reson **163**(1), 8 (2003). DOI 10.1016/S1090-7807(03)00153-8
25. K. Kobzar, T.E. Skinner, N. Khaneja, S.J. Glaser, B. Luy, J Magn Reson **170**(2), 236 (2004). DOI 10.1016/j.jmr.2004.06.017
26. T.E. Skinner, T.O. Reiss, B. Luy, N. Khaneja, S.J. Glaser, J Magn Reson **167**(1), 68 (2004). DOI 10.1016/j.jmr.2003.12.001
27. K. Kobzar, B. Luy, N. Khaneja, S.J. Glaser, Journal of Magnetic Resonance **173**(2), 229 (2005). DOI 10.1016/j.jmr.2004.12.005
28. K. Kobzar, T.E. Skinner, N. Khaneja, S.J. Glaser, B. Luy, J Magn Reson **194**(1), 58 (2008). DOI 10.1016/j.jmr.2008.05.023
29. K. Kobzar, S. Ehni, T.E. Skinner, S.J. Glaser, B. Luy, Journal of Magnetic Resonance **225**, 142 (2012). DOI 10.1016/j.jmr.2012.09.013
30. T.E. Skinner, N.I. Gershenzon, M. Nimbalkar, W. Bermel, B. Luy, S.J. Glaser, J Magn Reson **216**, 78 (2012). DOI 10.1016/j.jmr.2012.01.005
31. M.R.M. Koos, H. Feyrer, B. Luy, Magn Reson Chem **53**(11), 886 (2015). DOI 10.1002/mrc.4297
32. J.D. Haller, D.L. Goodwin, B. Luy, Magn Reson **3**(1), 53 (2022). DOI 10.5194/mr-3-53-2022
33. S. Slad, W. Bermel, R. Kümmerle, D. Mathieu, B. Luy, J Biomol NMR **76**(5-6), 185 (2022). DOI 10.1007/s10858-022-00404-1
34. D. Joseph, C. Griesinger, Science Advances **9**(45), eadj1133 (2023). DOI 10.1126/sciadv.adj1133
35. C. Buchanan, G. Bhole, G. Karunanithy, V. Casablancas-Antràs, A. Poh, B.G. Davis, J.A. Jones, A.J. Baldwin. Seedless: On-the-fly pulse calculation for NMR experiments (2024). DOI 10.1101/2024.01.31.578133
36. S. Ehni, B. Luy, Journal of Magnetic Resonance **232**, 7 (2013). DOI 10.1016/j.jmr.2013.04.007

37. S. Ehni, M.R.M. Koos, T. Reinsperger, J.D. Haller, D.L. Goodwin, B. Luy, Journal of Magnetic Resonance **336**, 107152 (2022). DOI 10.1016/j.jmr.2022.107152
38. K. Fehér, S. Berger, K.E. Kövér, J Magn Reson **163**(2), 340 (2003). DOI 10.1016/S1090-7807(03)00113-7
39. C.M. Thiele, W. Bermel, Journal of Magnetic Resonance **216**, 134 (2012). DOI 10.1016/j.jmr.2012.01.008
40. L. Kaltschnee, A. Kolmer, I. Timári, V. Schmidts, R. W. Adams, M. Nilsson, K. E. Kövér, G. A. Morris, C. M. Thiele, Chemical Communications **50**(99), 15702 (2014). DOI 10.1039/C4CC04217D
41. J. Furrer, M. John, H. Kessler, B. Luy, J Biomol NMR **37**(3), 231 (2007). DOI 10.1007/s10858-006-9130-x
42. J.R. Garbow, D.P. Weitekamp, A. Pines, Chem Phys Lett **93**(5), 504 (1982). DOI 10.1016/0009-2614(82)83229-6
43. D. Uhrín, T. Liptaj, K.E. Kövér, J Magn Reson A **101**(1), 41 (1993). DOI 10.1006/jmra.1993.1005
44. A.J. Shaka, C.J. Lee, A. Pines, Journal of Magnetic Resonance (1969) **77**(2), 274 (1988). DOI 10.1016/0022-2364(88)90178-3
45. B. Luy, K. Kobzar, T.E. Skinner, N. Khaneja, S.J. Glaser, J Magn Reson **176**(2), 179 (2005). DOI 10.1016/j.jmr.2005.06.002
46. Y.T. Woordes, B. Luy, (to be submitted)
47. L. Lerner, A. Bax, Journal of Magnetic Resonance (1969) **69**(2), 375 (1986). DOI 10.1016/0022-2364(86)90091-0
48. G. Mackin, A.J. Shaka, J Magn Reson A **118**(2), 247 (1996). DOI 10.1006/jmra.1996.0033
49. K.E. Kövér, V.J. Hruby, D. Uhrín, Journal of Magnetic Resonance **129**(2), 125 (1997). DOI 10.1006/jmre.1997.1265
50. W. Koźmiński, Journal of Magnetic Resonance **137**(2), 408 (1999). DOI 10.1006/jmre.1998.1700
51. B.L. Marquez, W.H. Gerwick, R. Thomas Williamson, Magnetic Resonance in Chemistry **39**(9), 499 (2001). DOI 10.1002/mrc.902
52. K. Kobzar, B. Luy, Journal of Magnetic Resonance **186**(1), 131 (2007). DOI 10.1016/j.jmr.2007.02.005